

## Fuzzy Control Vehicle-To-Grid Technology in a Micro-Grid using DC Fast Charging Architecture

R.Murali<sup>1</sup>, U.Chaithanya Kumar<sup>2</sup>, N.Spandana Goud<sup>3</sup>, Dr.T.Anil Kumar<sup>4</sup>

<sup>1,2</sup>Assistant Professor, Department of Electrical and Electronics Engineering, Anurag University, Hyderabad, Telangana, India.

<sup>3</sup>PG Student, Department of Electrical and Electronics Engineering, Anurag Group of Institutions, Hyderabad

<sup>4</sup>Professor, Department of Electrical and Electronics Engineering, Anurag University, Hyderabad, Telangana, India.

Email: <sup>1</sup>muraliee@cvsr.ac.in, <sup>2</sup>chaitanya.uddamarri@gmail.com, <sup>3</sup>goud.spandana08@gmail.com, <sup>4</sup>thalluruanil@gmail.com.

### ABSTRACT

As energy storage equipment in micro grids, the electric vehicle (EV) battery can be used. When the energy supply of granny-to-vehicle and G-V (Vehicle-to-Grid, V-G) exceeds the grid, and when demand is made available there is power supply back to the grid, micro grid energy control can be useful. In order to apply this technique, appropriate infrastructure and control systems need to be established. This report contains the design to create a V-G to G-V micro-grid system using fast charge of the EVs level 3. An EV interface micro-space testing system is modelled with a rapid loading station. Coordination is the control over the charging pattern of different EVs and their relative battery status in response to the present grid conditions. Good coordination between EVs is therefore needed to stabilise the grid. In light of the increased penetration of EVs, the vehicle-to-gage idea (V-G) can be researched in order to send the additional energy in controlled form back into the grid. Battery energy from EVs can be discharged into the grid as a distributed energy storage method by V-G in collaboration. The voltage profile at distribution nodes may be flattened if EVs are charged in a coordinated manner. A typical city distribution system is designed to exhibit V-G capacity, For example, high demand and reduced voltage. The simulation of the V-G distribution system is tested using the logic controller (FLC). In both the loading station controller and the V2G controller, two controls have been incorporated into the system. On the flow of electricity from the EVs to the grid, a collective decision is made. According to the real scenario in terms of energy or time required for the charge the power output of the EV network is being handled and tested.

**Key words** --- Electric, fast-paced DC, off-board loader, Grid inverter connected, smart grid, car-to-grid.

### 1. INTRODUCTION

Energy storage devices are a key component of the micro-grid, which permits the integration of intermittent renewable sources of energy to the grid. As long as the electric cars are charged, the microwaves can be used to store the automobiles. Most personal transport vehicles stay approximately 22 hours a day, and are an idle asset at that time. When surplus energy is present (Grid-To-Vehicle, G-V), EVs could perhaps improve micro-grid energy management by stocking energy and replenishing this energy when demand is met (Vehicle-To-Grid). V-whole G's power grid is facing obstacles such as control complications, a high number of EVs needed and difficult for short-term implementation[1]. The implementation of V-G in a micro-grid is easy in this circumstance. The V-G technology saves energy in electric batteries for vehicles and delivers that energy to the grid, wherever the grid managers request it. The fleet would provide significant energy storage for electric automobiles. The V-G approach can alleviate stress on overcharged distribution systems, like distributed energy resources, in particular during peak hours, by responding to demand at local level. Utilities grid operators can interact via a communication connection to connected autos. Providers can, when required, purchase electricity from car owners at low demand. An aggregator that acts as a business intermediary between the utility and several vehicles can be developed instead of communicating with individual vehicles[2]. Depending on the existing grid conditions, the aggregator is responsible for determining choices on the charging or unloading of EVs. In order to improve coordination and reliable operation, an aggregator can also be included to the smart grid[3]. A V-G system aggregator is displayed in Fig. 1.

Electric batteries from a regular outlet can be loaded from home. These increased electrical loads nevertheless generate a distortion of demand from supply, leading in turn to voltage and frequency instability. The distribution node may also raise voltage, even if it was suddenly discharged. Therefore, this two-way energy flow from the EVs to the grid needs to be appropriately controlled in order to ensure grid stability. Literature reveals that relatively little effort on controlling the issue of EVs and the grid has been done. An optimum aggregator [4], [5] was described in the use of EVs for frequency monitoring. A comparable piece of work is available in [6] where V-G integration has been studied in a Danish farm but energy storage is not V-G. In addition, the transmission network model has been established. The effects of EVs on the distribution grid were analysed in [7] and [8] and analysed using methods for load flow.

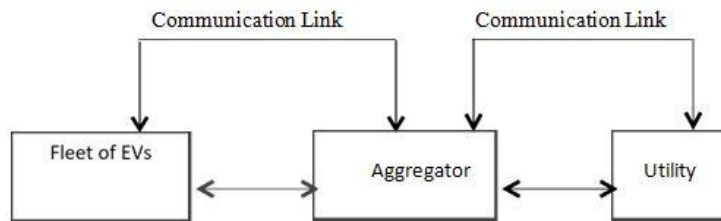


**Fig.1. Aggregator in V-G system.**

These works have, however, not utilised controlled methods for loading or unloading the power from the grid. The power flow control between the EV and the grid using FLC's for voltage corrective purposes was discussed in this article. Because it represents the rules linguistically, fuzzy control techniques were employed without developing a mathematical system model. Even if a huge number of EVs are involved, a control mechanism can be simple to create for their loading and discharge rates. Two controllers based on fluoridated systems were developed in this paper. The second controller termed the V-G controller here is located at the distribution node level (Fig. 2). This control is located at the loading station. Three charging levels of EVs are set by the Automotive Engineers Association. The charge of level 1 is connected to the on-board charger of the car using a plug and a regular household outlet (120 V). This is the slowest way for people who are under 60 kilometres a day and have to load overnight. Charging at level 2 needs a special Electric Vehicle Supply Equipment (EVSE) to supply 220 V, 240 V and up to 30 A electricity at home or at public service stations. The level of loading 3 is also known as quick load dc. DC quick-loaders provide loads of up to 90 kW at 200/450V, loading time reduction up to 20-30 min. A V2G micro grid architecture is ideal for DC fast charging since power transfer is needed swiftly for EVs used to store energy.

The V2G controller's major objective is to govern the flow of the electricity between the node and the charging station. At the distribution node there is a charging station, supposed to be a significant pool of EVs from this specific area. This charge station is fitted with the second controller, the loading station controller. The controller shall decide for the loading or unloading of the EVs individually. Coordinated loading or unloading of EV's has been shown to allow V2G technology to fulfil voltage decrease, power imbalance and other auxiliary services, such as frequency regulations and transient reduction. This study has been examined in detail on peak power management and voltage stability.

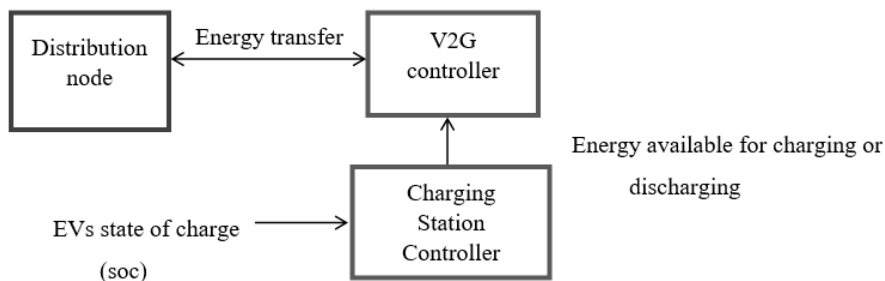


**Fig. 2. Controllers implemented in V-G infrastructure.**

The level 1 and level 2 ac charges[3] in V-G technology are used for majority of the works described. The on-board charger power rating limits certain charging solutions. Another problem is that it was not designed in the distribution system for bidirectional energy flow. In this case, research is required to design technically viable charging station structures for V-G micro-grid technologies. This study offers an infrastructure for dc fast charging systems in a micro-grid system with V-G capability. The dc bus for interfacing EVs also allows the integration into the micro-grid of a solar photovoltaic array (PV). The suggested architecture offers high-performance two-way recharging for EVs by off-board

loaders. For both V-G and G-V modes, MATLAB/Simulink simulations are used to determine the effectiveness of the recommended model.

2. EV's SYSTEM MODELING

2.1 EV's battery modelling

The following assumptions were considered in the modelling of the EV battery. Cyclic battery efficiency is not taken into account.

- Loss of capacity of the battery for cycling is not taken into account.
- Voltage variation is not addressed in relation to SOC.

This article focuses on showing grid support via EVs. The assumptions above are set so that the calculation time is reduced. The battery is considered as a source for supplying power required for the unloading process as a result of these assumptions. The battery is modelled as a sink that can absorb power from the grid when charged.

2.2 Grid support usage of EVs

The EV battery energy can be used as a distributed energy storage, for reactive electricity supply, and to reduce the voltage pitch at a particular node. Fig. 3 depicts a battery system with an X line distribution node bidirectional transformer.

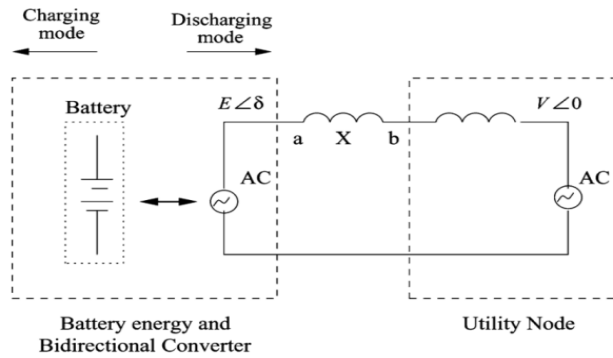


Fig. 3. Batteries used as a distributed source of energy.

A distribution node exists. The energy available from the charging station in the following figure is shown by the battery. This battery may either be a source or a two-way converter platform for collectively discharging or charging vehicles at the charge station. The transformer is connected to a power battery and synchronised to the network system. At point B of the connection, the injection power battery consists of the power supply. Storage power of the battery may be written accordingly

$$S_{EV} = VI \tag{1}$$

Where,

$$I = \frac{E\delta - V}{jX} \tag{2}$$

$S_{EV}$  and is supplied correspondingly by battery power and current in (1) and (2). E and Display tensions at the sending and receiving ends. • E and V corner. X is the line response to the converter's utilities node. The battery power system replaces I and 's value between real and imagined elements as follows:

$$S_{EV} = \frac{EV \sin \sin(\delta)}{X} + j \frac{E\{E - V \cos \cos(\delta)\}}{X} \tag{3}$$

The reactive power of P EV real and Q EV are indicated below in (3).

$$P_{EV} = \frac{EV \sin \sin(\delta)}{X} \tag{4}$$

$$Q_{EV} = \frac{E\{E - V \cos \cos(\delta)\}}{X} \tag{5}$$

The angle  $\beta$  in the phase and voltages are E and V if reactive power is to be injected only with an EV. At the end of the transmission the activated and reactive power is replaced as follows by  $\dot{S}=0$ in (4) and (5):

$$P_{EV} = 0 \tag{6}$$

$$Q_{EV} = \frac{E^2 - EV}{X} \tag{7}$$

Thus, EVs can support reactive power via converters. The converter is adjusted so that the phase angle from E and V to low voltage reactive power is 0 at all times. The angle of high voltage correction must be modified to inject both actual and reactive power in the appropriate node. As this study aims to prove grid support concept solely for real power injections, 0.9 for all charging and unloading systems will be assumed. A power factor of 0.9 Electricity is drained out of the grid during off-peak hours to improve the voltage and charge. During the charging procedure, the grid's power usage is nil.

### 2.3 Battery charger configuration

To facilitate speedy loading, the loaders are located off-board and in EVSE position. A two-way dc-dc converter provides the basic building block for an off-board V-G charger. The EV and DC distribution networks are connected. On Fig. 4, you can see how to configure the converter. Using IGBT / MOSFET, it always tests two switches.

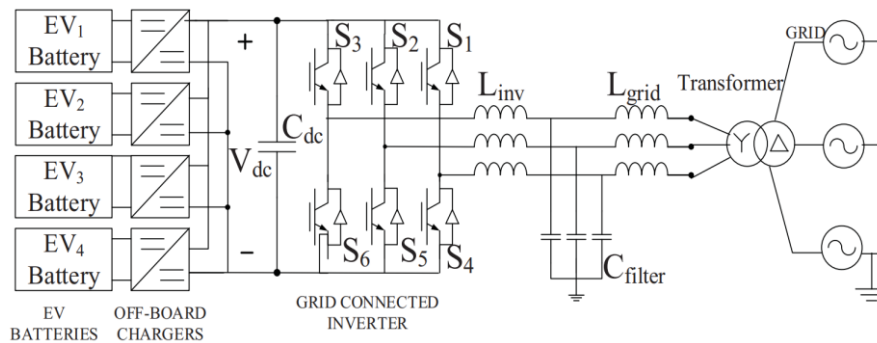


**Fig. 4. EV charge station for quick dc load.**

Buck operation mode (charging mode): when the S Buck is top switch works, the converter serves as an input buck converter that decelerates the V dc to V battery charging voltage. The current passes via the switch and inducer to the battery during the on state. This is the charge process where the flow of power from the vehicle's grid is (G-V). The current travels its return route via the lower switch's inductive and diode and completes the circuit when the switch is off. When the battery voltage is specified by the duty ratio of the upper switch:

$$V_{batt} = V_{dc} * D \tag{8}$$

Open mode: Converts V to Vdc batteries when the lower S boot is present. An antiparallel diode in the top and condenser switches allows current to flow continuously through the pulse once the switch is triggered. Vehicle to grid power flow (V-G) when the battery discharges. As long as the capacitor is large enough to provide a stable DC voltage, the output voltage will be adequate.

$$V_{dc} = \frac{V_{batt}}{1-D^1} \tag{9}$$

Which is the bottom switch's duty cycle.

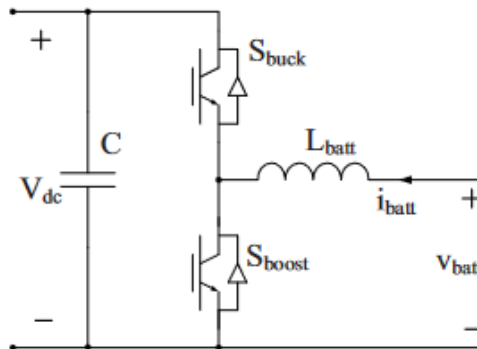


**Fig. 5. Battery charger configuration**

**2.4 Filter and inverter**

The grid-connected inverter (GCI) converts the DC bus's tension into a three-stage ac voltage that facilitates the flow of current via the buttons' parallel diodes. It is connected to each GCI leg by way of a grid (Fig. 5). The output terminals are coupled to an LCL filter to reduce harmonic voltage and pure sinusoidal voltage. For this task, design techniques have been developed to determine the LCL filter parameters[4].

**3. CONTROL SYSTEM**

Control the off-board loader For charging/discharge control of the battery charge circuit, a continuous current control approach [5] is applied utilising FLC controllers, shown in Fig. 6. The controller first measures the battery reference current against zero in order to calculate the polarity of the current signal and selects between charging and download processes. When selection of the mode and an FLC controller is used for the error to generate the pulses switching for S boost/S buck, the reference current is compared to the measured current. S boost will be switched off while loading and S buck will be shut down during downloading.

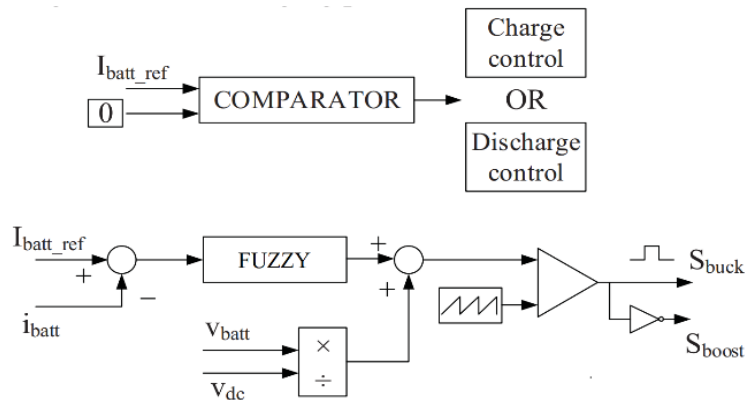


**Fig. 6. Current Battery Charger Control Strategy Inverter Control**

In the synchronous reference framework, the inverter controller has a cascade control. Fig.8[4] displays the usual two PI and two Nest loop FLC standard vector control. Two external voltage control loops and two internal current control loops are included in the control architecture. D-axis loop controls dc bus voltage and current. Similar to the inner current loop, the q-axis outer loop modifies AC voltage by altering the reactive current. To further boost transient performance, both L and forward voltage signals are employed.

**4. FUZZY LOGIC CONTROLLER BASED V2G INFRASTRUCTURE**

Uncoordinated power loading or discharge of transmission networks may change the voltage profile of the nodes, e.g., uncoordinated loading and discharge of energy power supply may increase or decrease node voltages over the standard CEA. The frequency and frequency is controlled by the application of a fluid logic check in this study (FLC). For instance, at the loading station, Each vehicle shall take the entry parameters as current SOC's and voltage profiles. EV loads for high and low SOC voltages, EV loads for a high SOC voltage and a low node. However, both high and low SOC and node voltages. However, it may also occur. A controlled charge or discharge rate must be used for such scenarios. The FLC is thereforewell adapted to deal with these conditions, so that node voltage variations are maintained within the necessary standards.

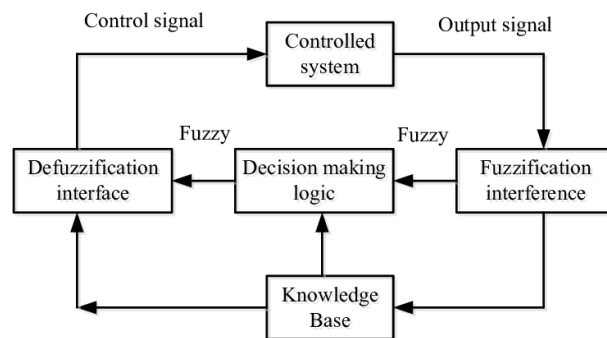


**Fig. 7: FLC system.**

### 4.1 Fuzzy Foundations of Logic Controller

Unlike binary logic, fuzzy logic is a logic that allows for real values between 0 and 1 for fuzzy logic variables. Due to a straightforward IF-THEN regulatory approach, fugitive logic can deal with system insecurity and bypass the system mathematical model requirement. In sophisticated systems which are not fully presentable as a mathematical model, this is very useful. However, the raging logical complexity of the system is rapidly rising with a bigger number of inputs and outputs. This paper was developed for the FLC type Mamdhani [14].A FLC consists of four major components as shown in Fig. 7, flushing interface, rule base, logic of inferences, and interface of de-fuzzification. The fluzzifying interface turns binary logic entries into floating variables and the fluzzy version converts them into a binary logic output using the defuzzifying interface. There is an affiliation function. The rule is based on a collection of rules that set forth the method to control. For every output function, the output of each rule is obtained from the reducing logic[15]. The fuzzy centroid is then determined to achieve the binary output value of the composite area of output membership characteristics[16][17].

### 4.2 V-G controller design with Fuzzy

There are two stages in the design of the system. The charging station is on the first floor and the distribution node is on the second. The CSC selects whether to load or discharge the EVs separately by loading the station controller. The CSC input parameters are SOC and current node voltage for each vehicle battery. As shown in Figure 8, CSC produces all grid-supporting energy from the charging station depending on SOC's and the current status of each car. Similarly, net energy flows from grid toward charging station provide positive energy production, while net energy flows from grid toward charging station produce negative energy production.

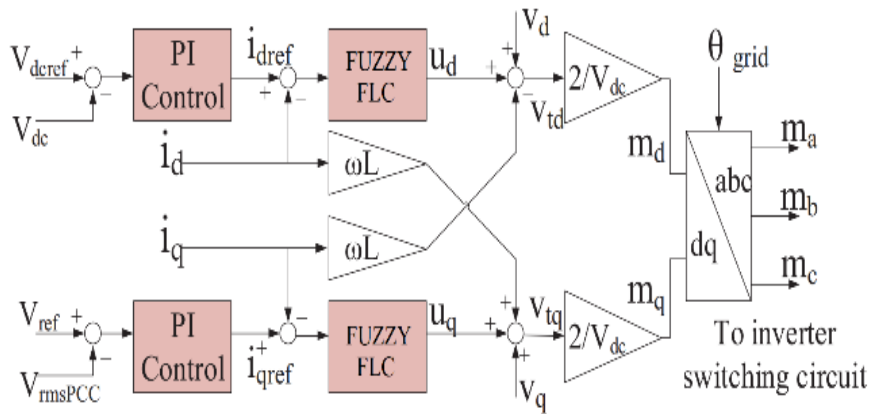


Fig. 8. Inverter control system.

Each vehicle can charge or discharge but depends only on its net energy flow to indicate the total output energy. Depending on whether nodal voltages must be increased or decreased, either a positive or negative power output is required for the application. As a distribution node's second controller, known as the V2G controller, is positioned immediately behind the central processing unit (CSC). On the basis of the information provided by the CSC, the V2G controller determines the energy flow into and out of the node at the charging station. As Fig. 8 shows, a summary block comes with the energy from the CSC. The actual node energy value is the second contribution in this summary section. This summing block has a net power output that takes into account battery energy and grid energy. This net power is sent to the V2G controller as the input, while the current voltage of the node is the other V2G input parameter. The V2G controller releases or deletes node power. This power output is adversely affected by the energy supply from the CSC if the charging station is a source of electricity. Positive efficiency means a charging station, i.e., when the CSC's energy efficiency is a negative one.

This agreement was adopted to give negative feedback on the summary block grid power. In this work, our model loader unit with three SOC levels was simulated instead of having the potential SOC levels "n" expected to save time.

TABLE I: CONTROLLERS NOTATIONS

CSC		V2G	
Operation Mode	Output Energy	Operation Mode	Output Power
Charging	Positive	Source	Negative
Discharging	Negative	Load	Positive

The output of the V2G controller as depicted in Fig. 8 controls the power flux from the EV to the grid in the sub-feeder. (PQ point). (PQ point). This PQ node is the final node for high voltage and load control. The fluctuation of the member functions depends heavily on the member's format. To improve calculations, input and output membership functions triangular membership functions are utilised. The minimum function used by Mamdani (sometimes referred to as the Max-Min inference method) is the rule. Determination is done with the approach of the centre of gravity. The problem is to determine the centre of the region, which includes and is mathematically defined by all rules

$$u(t) = \frac{\sum_{i=1}^n u_i \mu_v(u_i)}{\sum_{i=1}^n \mu_v(u_i)} \quad (10)$$

In  $\mu(t)$  a standardised control output is represented by  $\mu$  and a  $\mu v$  refers to the output variable. Five linguistic variables flow into input voltage: low, medium (M), medium (V), high (H), high, and high (VL) (VH). In 10 linguistic variables, the input energy is changed: The following: High negative effects (VNH), high negativity (NE), medium negative inputs (NM), low negative (NL) and very low positive inputs (VNL) (VPH). The fusion results are integrated into those areas represented by language variables: highly negative (VNH), highly negated (NH), negative medium (VNM), Negative (NM), low negative (NL) and very negative (VNL) (VPH).

The voltage and SOC are both inputs for the load station controller and the power output is the energy utilised for the construction of similar membership functions.

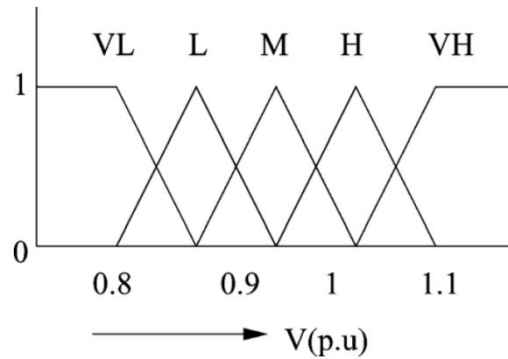


Fig. 9. Fuzzy membership function (voltage).

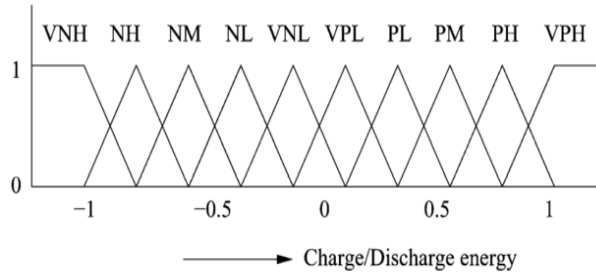


Fig. 10. Fuzzy membership function (energy).

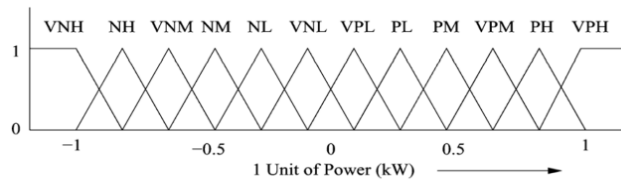


Fig. 11. Fuzzy membership function-load/source of EV battery.

TABLE II :RULES FOR V2G CONTROLLER:

E/V	VL	L	M	H	VH
-----	----	---	---	---	----

VNH	VPL	PL	PM	VPM	PH
NH	VPL	PL	VPM	PH	VPH
NM	VPL	PL	PM	VPM	PH
NL	VPL	PL	PM	PH	VPH
VNL	VPL	PL	VNL	NL	NM
VPL	VNL	VNL	NL	PL	VPL
PL	VNL	NL	NM	NM	VNM
PM	VH	VNH	NM	NL	VNL
PH	VNH	NH	NM	NL	VNL
VPH	VNH	NH	VNM	NL	VNL

Figures 9, 10, and 11 show the membership functions for V2G controllers. Table III provides the rule base for V2G controllers, whereas 'E' refers to energy and 'V' refers to voltage. Fig. 12 also shows the fluctuating CSC membership functions. The V2G controller has comparable membership functions for power and voltage.

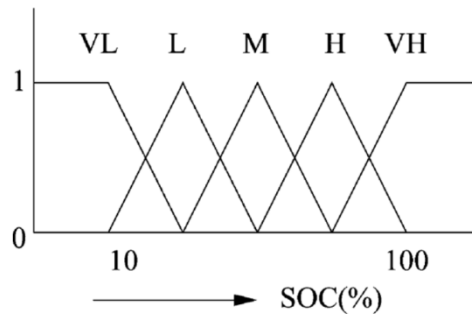
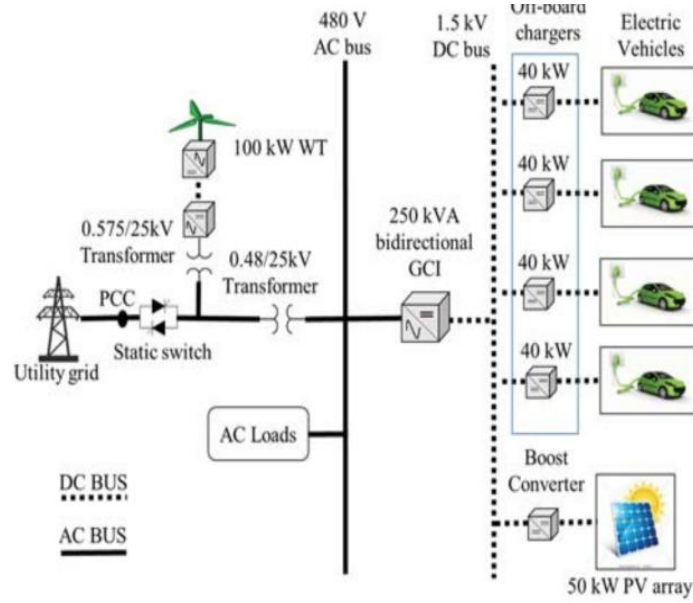


Fig. 12. Fuzzy membership function (SOC).

### 5. MICRO-GRID TEST SYSTEM CONFIGURATION

Fig.13 shows the configuration of the micro-grid assay system for a quick loading station dc. A 100kW wind turbine is generated by the wind turbine (WT) and the solar PV array. The EV batteries have 4 EV battery and are connected via the off-board charges via a 1.5 kV dc bus to the charging station. A boost converter with the MPPT controller additionally connects the PV from the Solar Panel to the dc bus. The grid consists of a distributor of 25 kV and a transmission system equivalent to 120 kV. The double-feed wind turbine induction generator at the location of the common interconnection is linked to the micro-grid (PCC). For voltages increase and link the respective ac system to the grid, transformers are needed.





**Fig. 13. Proposed microgrid test system configuration.**

**6. RESULTS**

The analysis of V2G with FLC for loading and discharging of EVs was reported in the preceding section. Results from the preceding part are shown in this section to fulfil the high demand. Two scenarios constructed in Section V investigate the loading and unloading behaviour of the EV during peak and off-peak periods. Flattening of the charging profile by means of simulation results is shown in the concluding portion of this section. The technique for designing charging stations is changed from [4] and the acquired parameter values are presented in the appendix. With a maximum power output of 100 kW the wind turbine has a rated speed. Solar PV is operated under typical settings in which it has a maximum output of 50% (i.e. 1000W/m<sup>2</sup> irradiation and 25°C temperature). The 480 V ac bus has a 150 kW resistive load. For operation of unit Pf the current reactive reference to GCI is set to nil. The EV battery's initial charging status (SOC) is set at 50%. After stable conditions are fulfilled, EV1 and EV2 batteries (Fig. 4) are operated to transfer power from the V-G to the G-V. Table III shows the current configuration for the EV1 and EV2 battery charging circuits and the following figures illustrate the results of this measurement.

**TABLE III: CURRENT SET-POINTS TO EV BATTERIES:**

Time range(s)	0 to 1	1 to 4	4 to 6
Current set-point to Ev1 battery(A)	0	+80	0
Current set-point to Ev2 battery(A)	0	0	-40

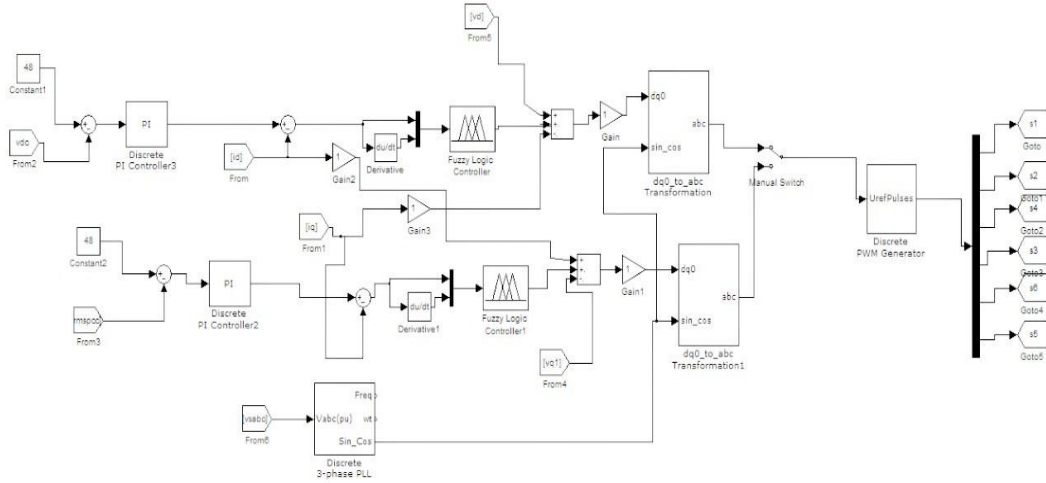


**Fig 14. Simulink model for proposed controller.**

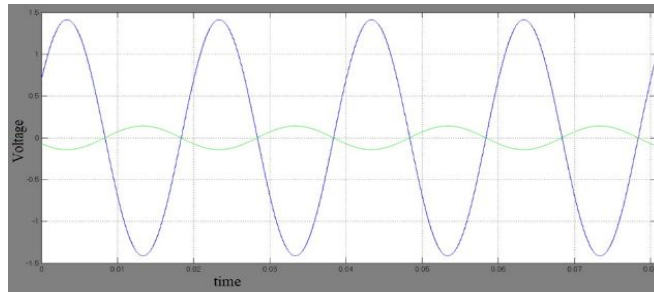


**Fig. 15. During the V-G operation, waveform refers to grid voltage and grid injected current.**

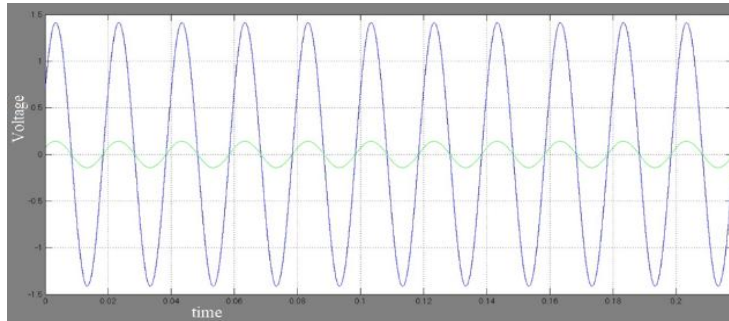


**Fig. 16. During operation with G-V waveform represent the grid tension and the injected grid current.**

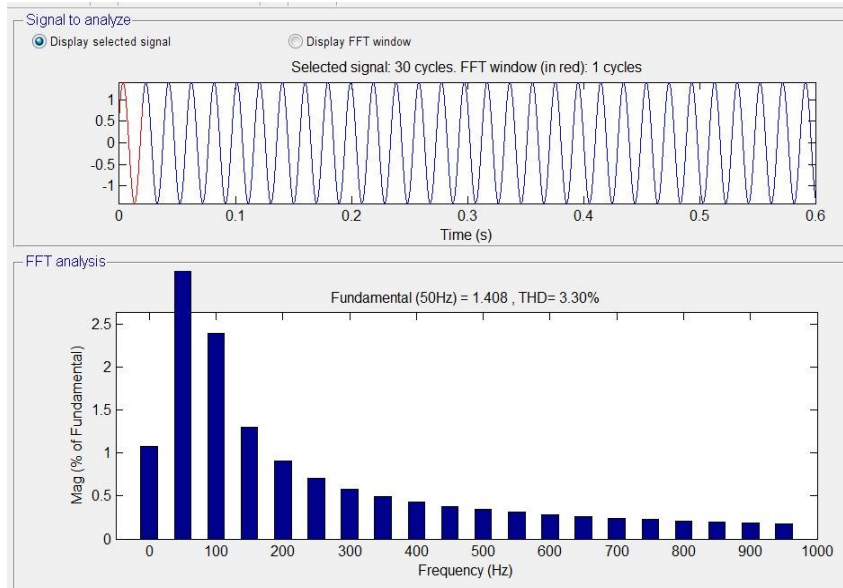


**Fig. 17. PI controller harmonic spectrum and THD of grid injected current.**

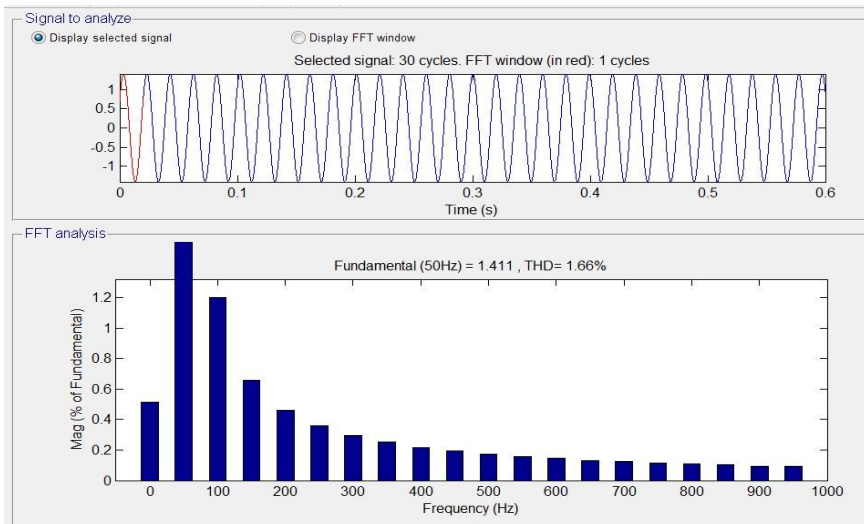


**Fig18.Harmonic spectrum and THD grid injected current fuzzy logic controller.**

Fig. 15 demonstrates, during the V-G operation, the grid voltage and grid injected current are 180 degrees out of phase during v2g operation and this shows the reverse power flow. Fig16.demonstrates, the grid voltage and grid injected current are in phase during g2v operation. Fig17.demonstrates, by using pi controller, the total harmonic distortion of grid injected current is obtained as 3.3%. Fig. 18demonstrates, by using fuzzy logic controller, the total harmonic distortion of grid injected current is obtained as 1.66%. Fig. 19 demonstrates, during the time period of 0.1 sec to 0.4 sec,

- The battery percentage is decreased from 48.3% to 48.1% Which means it releases some amount of current.
- The current is increases from 0A to 80A.
- The voltage is decreases from 540v to 510v.

Fig. 20 demonstrates, during the time period of 0.4 sec to 0.55 sec,

- The battery percentage is increased from 50% to 50.05% which means, it stores some amount of current.
- The current is decreased from 0A to - 40A.
- The voltage is increased from 539v to 545v.

Voltage

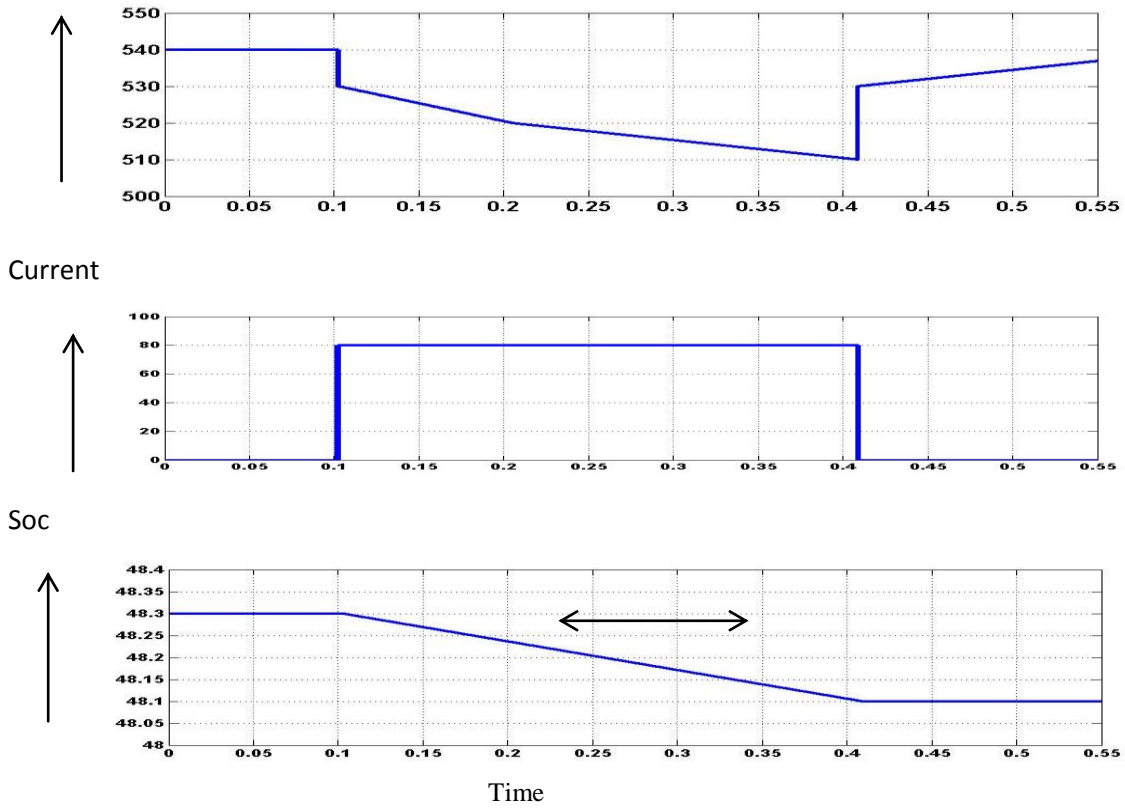
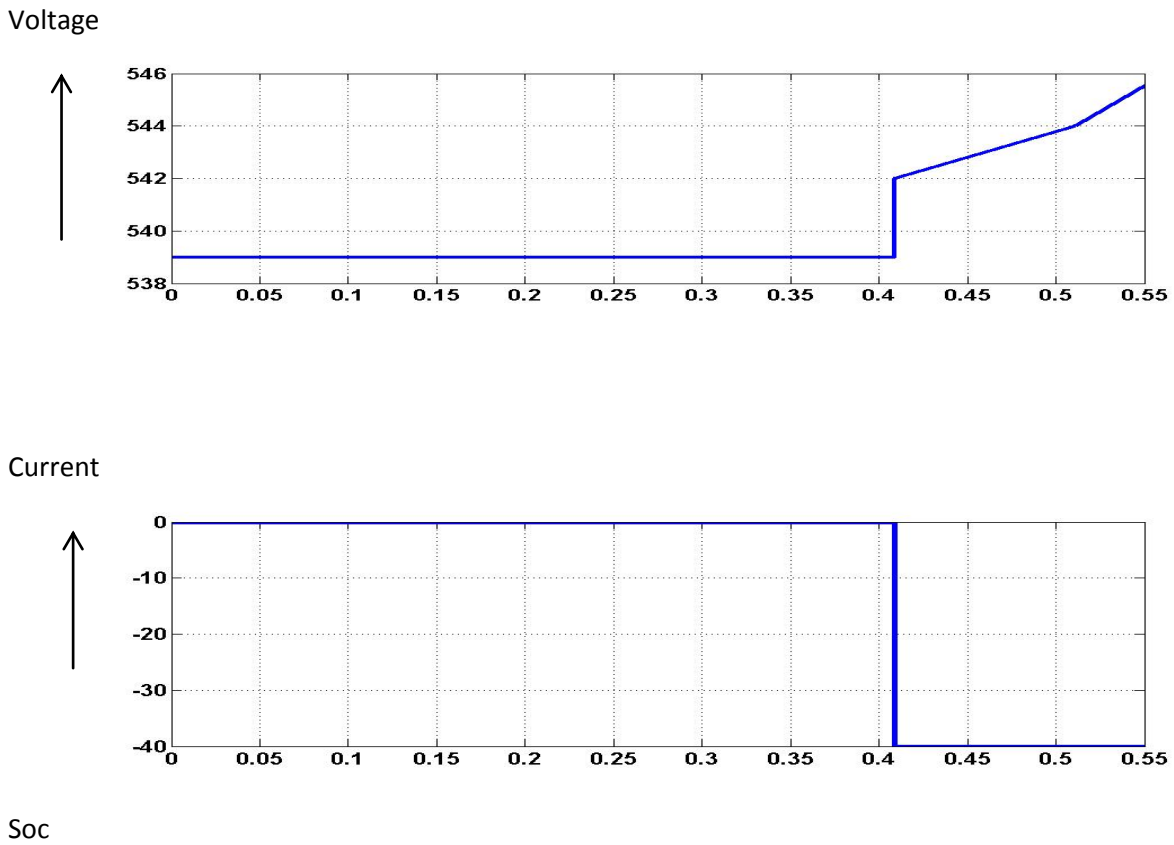
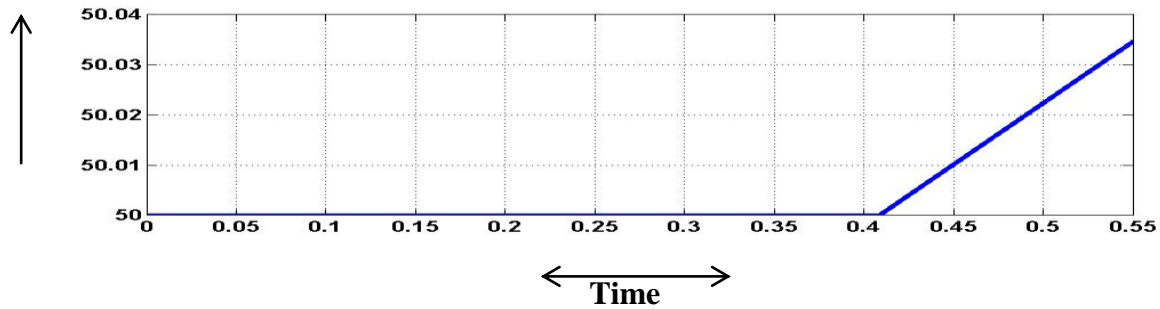


Fig. 19. This waveform represents grid voltage and grid injected current and soc of electric vehicle battery during v2g operation





**Fig. 20.** This waveform represents grid voltage and grid injected current and soc of electric vehicle battery during g2v operation.

## 7. CONCLUSION

This document shows the modelling and design in a micro-grid of a V-G system employing a quick loading architecture. The interface between the EVs to the Micro-grid is created using a dc rapid charge station with off-board charger and a grid inverter. This power electronic interface control technology permits a two-way transmission of electricity between electrical devices and the grid. Using Fuzzy Logic the V-G control and loading station controller were developed. These controls were used to govern the energy flow between electrical transmission units and the grid. The FLC was created for the operation V-G in relation to voltage stability and peak demand control and the influence of this V-G operation was analysed for two different situations. EVs can be loaded and discharged using an FLC effortlessly, as demonstrated by the simulation results. EVs for power elevator and peak savings can be charged over off-peak times and electricity discharged at peak times. We are working to expand this concept by taking into consideration additional variables such as:

- Charging and unloading should be carried out on the basis of the current prices and battery.
- V2G is employed in the dynamic and steady state for the voltage control and sag support.

## REFERENCES

- [1] J. Tomic and W. Kempton, "Using fleets of electric-drive vehicles for grid support," *J. Power Sources*, vol. 168, pp. 459–468, 2007.
- [2] G. G. C. Guille, "A conceptual framework for the vehicle-to-grid (V2G) implementation," *Energy Policy*, pp. 4379–4390, 2009.
- [3] W. Kempton and J. Tomic, "Vehicle-to-grid power implementation: From stabilizing the grid to supporting large-scale renewable energy," *J. Power Sources*, vol. J144, pp. 280–294, 2005.
- [4] S. Han, S. Han, and K. Sezaki, "Development of an optimal vehicle-to-grid aggregator for frequency regulation," *IEEE Trans. Smart Grid*, vol. 1, no. 1, pp. 65–72, Jun. 2010.
- [5] K. Shimizu, T. Masuta, Y. Ota, and A. Yokoyama, "Load frequency control in power system using vehicle-to-grid system considering the customer convenience of electric vehicles," in *Proc. Int. Conf. Power Syst. Technol. (POWERCON)*, Oct. 2010, pp. 1–8.
- [6] J. Pillai and B. Bak-Jensen, "Integration of vehicle-to-grid in the western Danish power system," *IEEE Trans. Sustainable Energy*, vol. 2, no. 1, pp. 12–19, Jan. 2011.
- [7] K. C. Nyns, E. Haesen, and J. Driesen, "The impact of charging plug-in hybrid electric vehicles on a residential distribution grid," *IEEE Trans. Power Syst.*, vol. 25, no. 1, pp. 371–380, Feb. 2010.
- [8] M. Singh, I. Kar, and P. Kumar, "Influence of EV on grid power quality and optimizing the charging schedule to mitigate voltage imbalance and reduce power loss," in *Proc. 14th Int. Proc. Power Electron. Motion Control Conf. (EPE/PEMC)*, Sep. 2010, pp. T2-196–T2-203.
- [9] NERLDC, North Eastern Load Dispatch Centre Shillong India [Online]. Available: <http://www.nerldc.org>
- [10] ASEB, Assam State Electricity Board. Guwahati, India [Online]. Available: <http://aseb.in/>, 2011
- [11] M. Baran and F. Wu, "Network reconfiguration in distribution systems for loss reduction and load balancing," *IEEE Trans. Power Del.*, vol. 4, no. 2, pp. 1401–1407, Apr. 1989.

- [12] M. Baran and F. Wu, "Optimal sizing of capacitors placed in a radial distribution system," *IEEE Trans. Power Del.*, vol. 4, no. 1, Jan. 1989, pp. 735–743.
- [13] "Energy storage and its usage with intermittent renewable energy," *IEEE Transactions on Energy Conversion*, vol. 19, no. 2, June 2004, pp. 441–448, by James Barton and David Infield.
- [14] Kluwer, 1991. H. Zimmermann, *Fuzzy Set Theory and Its Applications*.
- [15] A selection of papers by Lotfi Asker Zadeh, by G. J. Klir and B. Yuan, in *Fuzzy Sets, Fuzzy Logic, and Fuzzy Systems: Selected Papers*. World Scientific, Singapore, 1996.
- [16] (II) Fuzzy logic controller. 16 C. Lee "Fuzzy logic in control systems: Fuzzy logic controller." *IEEE Transactions on Systems, Man, and Cybernetics* 20 (2): 419–435.
- [17] "Intelligent Systems And Control Principles And Applications" by L. Behera et al Oxford University Press, Oxford, U.K., 2009
- [18] Assam Electricity Grid Corporation Ltd. Design Department [Online]. 1024.html is available at <http://www.aegsldc.org> in 2010.
- 2nd edition of *Fuzzy Logic With Engineering Applications*, by T. J. Ross.
- [20] A micro-grid construction and simulation study by Shumei C., Xiaofei L, Dewen T, Qianfan Z and Liwei S, published in *Proceedings of the International Conference on Electrical Machines and Systems, ICEMS 2011, 2011*, pp. 1–4.
- [21] S. Han, S. Han, and K. Sezaki, "Development of an optimal vehicle-to-grid aggregator for frequency regulation," *IEEE Trans. Smart Grid*, vol. 1, no. 1, pp. 65–72, 2010.
- [22] M. C. Kisacikoglu, M. Kesler, and L. M. Tolbert, "Single-phase on-board bidirectional PEV charger for V2G reactive power operation," *IEEE Trans. Smart Grid*, vol. 6, no. 2, pp. 767–775, 2015.
- [23] A. Arancibia and K. Strunz, "Modeling of an electric vehicle charging station for fast DC charging," in *Proceedings of the IEEE International Electric Vehicle Conference (IEVC)*, 2012, pp. 1–6.
- [24] K. M. Tan, V. K. Ramachandramurthy, and J. Y. Yong, "Bidirectional battery charger for electric vehicle," in *2014 IEEE Innovative Smart Grid Technologies - Asia, ISGT ASIA 2014, 2014*, pp. 406–411.
- [25] Bhatti, A.R.; Salam, Z.; Aziz, M.J.B.A.; Yee, K.P.; Ashique, R.H. Electric vehicles charging using photovoltaic: Status and technological review. *Renew. Sust. Energy Rev.* 2016, 54, 34–47.